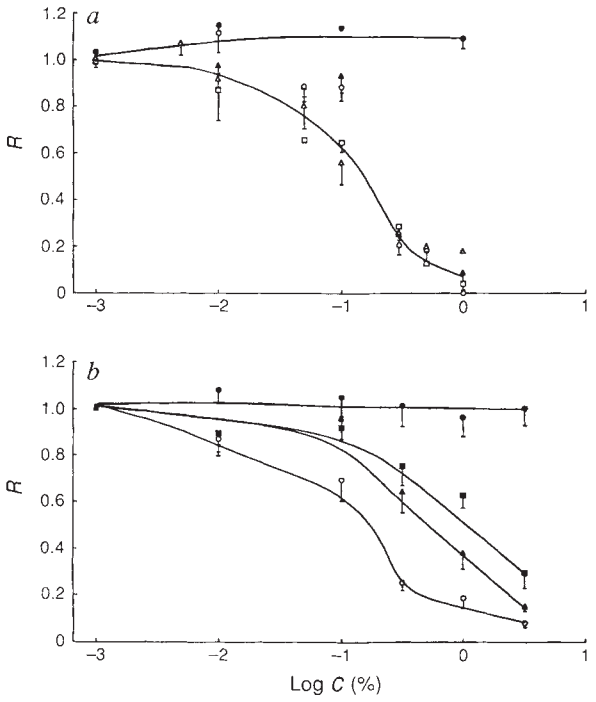

Effects of PA–LG on the taste nerve responses in frogs (*a*) and taste sensation in humans (*b*) to quinine hydrochloride (○), L-leucine (□), caffeine (△) and papaverine hydrochloride (▲), L-isoleucine (■) and NaCl (●). *R* in the ordinate represents relative magnitude of taste sensitivity.

figure (*a*). Responses to bitter substances are decreased with increased concentration of PA–LG to a level of 1 per cent, while the response to NaCl is unaffected by all concentrations of PA–LG examined. These results indicate that high concentrations of PA–LG completely suppress the bitter responses by full occupation of the receptor sites. The data obtained with four bitter substances roughly follow a single curve, suggesting that if there are multiple receptor sites for bitter substances, PA–LG binds uniformly to them.

We also examined the effects of PA–LG on taste sensation in humans to bitter substances by a psychophysical method. For usefulness in practical application, the tongue was not pretreated with PA–LG, but subjects tasted bitter substances dissolved in solutions containing PA–LG of varying concentrations. Standard solutions containing different concentrations of bitter substances and no PA–LG were prepared and the subjects were asked to choose a standard solution whose bitterness is equivalent to that of a test solution. The figure (*b*) shows that the bitter tastes of quinine hydrochloride, papaverine hydrochloride and isoleucine are suppressed by PA–LG, whereas the salty taste of NaCl is unaffected. We emphasize that PA–LG is useful for masking bitter tastes of drugs and foods, and also for exploring characteristics of the receptor sites for bitter taste.

Yoshihisa Katsuragi*
Kenzo Kurihara
Faculty of Pharmaceutical Sciences, Hokkaido University, Sapporo 060, Japan
**Kao Corporation, Kashima, Japan*

Death of an ice sheet

SIR — The Barbados and New Guinea records of sea-level history suggest that there were two massive glacial-meltwater inflows during the past 15,000 years[1–3]. The timing of these inflows relative to other environmental changes (such as changes in North Atlantic deep water (NADW) circulation) figures prominently in efforts to understand the last glacial to interglacial climate transition and the Younger Dryas event[4]. According to prevailing oceanographic theory, the magnitude of the first inflow was large enough to have shut down NADW circulation, thereby initiating colder climates in Europe (for example the Younger Dryas event)[5]. We have conducted ice-sheet modelling experiments which suggest why there were two massive, but short-lived, inflows of glacial meltwater as opposed to a single, more gradual influx[6,7]. In particular, our simulations identify the first meltwater influx event (approximately 14,000 calendar years ago) with the collapse of the Eurasian ice sheet (EIS), a marine ice sheet that covered Scandinavia and the Barents, Kara and Laptev seas[8].

Our simulations determined a steady-state initial configuration of the EIS associated with estimated glacial-maximum climate. The modelled EIS was then forced to retreat according to a prescribed atmospheric-warming schedule indexed to a simplified atmospheric-CO_2 chronology derived from the Vostok ice core[9]. (The Vostok ice-core record and our assumptions concerning its relevance to climate conditions over the EIS determined the timing of EIS retreat in the simulation.) The figure compares the observed and simulated meltwater-inflow histories, Q_o and Q_m, respectively. Both histories display a peak that occurs approximately 14,000 calendar years ago. (Recent comparisons[3] between the Barbados and New Guinea sea-level records suggests that uncertainty in the timing of this peak is approximately 1,000 years.) The peak in Q_m is larger (by approximately 50 per cent) and more recent (by 500 years) than that in Q_o. When we conducted our simulations, we knew nothing about the Barbados or New Guinea sea-level histories; thus, our simulations were not fine-tuned to reduce the volume of the initial EIS configuration needed for better agreement between Q_o and Q_m. Although our model did not address the Laurentide ice sheet (LIS), we infer that the second pulse in Q_o (at approximately 11,000 years ago) represents the demise of the LIS.

We attribute the rapidity of sea-level rise achieved by our model to the acceleration of ice-sheet flow towards iceberg-calving margins, rather than to a process of enhanced ice-sheet surface melting. This acceleration is caused by the retreat of grounding lines (boundaries between floating ice shelves and grounded ice sheets) into regions of isostatically depressed bedrock topography. Retreat into regions of lower bedrock elevation reduces friction which restrains seaward ice flow and, at the same time, increases (locally) the stresses which drive this flow. Ice-sheet mechanics may thus account for the unanticipated strength and brevity of the two meltwater pulses seen in the sea-level record.

Our model cannot explain why the demise of the LIS was delayed for 2,500

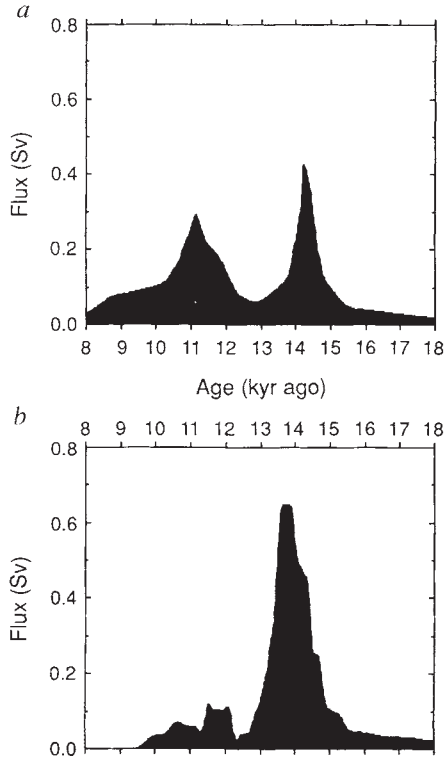

a, Observed history of meltwater influx[1–4]; *b*, modelled history of meltwater influx due to EIS collapse[6,7].

© 1993 Nature Publishing Group

years or so following the collapse of the EIS (see figure). Perhaps this delay was a result of transatlantic asymmetry in the climate system, a higher tolerance of the LIS to climate warming, or the effects of short-lived cooling perturbations possibly caused by the first meltwater influx (such as Younger Dryas cooling).

1. Fairbanks, R. G. *Nature* **342**, 637–642 (1989).
2. Bard, E., Hamelin, B., Fairbanks, R. G. & Zindler, A. *Nature* **345**, 405–410 (1990).
3. Edwards, R. L. *et al. Science* **260**, 962–968 (1993).
4. Charles, C. D. & Fairbanks, R. G. *Nature* **355**, 416–419 (1992).
5. Stocker, T. F. & Wright, D. G. *Nature* **351**, 729–732 (1991).
6. Lindstrom, D. R. *Paleoceanography* **5**, 207–227 (1990).
7. Lindstrom, D. R. & MacAyeal, D. R. *Science* **245**, 628–631 (1989).
8. Lehman, S. J. *et al. Nature* **349**, 513–516 (1991).
9. Barnola, J. M., Raynaud, D., Korotkevitch, T. S. & Lorius, C. *Nature* **329**, 408–413 (1987).

Dean R. Lindstrom
Sullivan East High School,
7677 South Coles,
Chicago, Illinois 60649, USA
Douglas R. MacAyeal
Department of Geophysical Sciences,
University of Chicago,
5734 South Ellis Avenue,
Chicago, Illinois 60637, USA

Recording fires by satellite

SIR — Cahoon *et al.*[1] illustrate the use of a satellite in mapping grass or forest fires at night. The wavelength band used was 0.4 –1.1 μm, which spans the visible and very near infrared part of the spectrum. The illumination of cities was eliminated by their permanence, fires being of short duration. Only photographic prints, and not the basic digital information, were archived. The satellite used was one of the Defense Meteorological Satellite Program (DMSP) Block 5, with an effective resolution of about 2.7 km.

Routine National Oceanic and Atmospheric Administration (NOAA) meteorological satellites seem more suitable in principle for this task, for every part of the Earth is traversed twice every 24 hours, in midday sunshine and at night. The intensity of sunshine is a maximum at 0.5 μm (corresponding to a temperature of 6,000 K) and the Earth's emission has a maximum at about 11.0 μm (300 K). These two emission spectra cross over with an intensity of about one-fortieth of the maximum at a wavelength of about 4 μm, the precise values depending on the emission temperatures and other factors. The satellite messages are in archives at the University of Dundee and are generally available.

The NOAA satellites record the scene below them in several wavebands, one of which, channel 3, is 3.55–3.93 μm. This is about the maximum strength in the emission spectrum for a temperature of about 700 K, or dull red heat. Flames at 1,200–1,500 K are about 16 times as intense although in channel 3 the strength is around half the maximum and so they can be 5 or 10 times as strong as red heat. But a flame with an area of only 20×20 m will outshine 1 km^2 of ordinary territory in bright sunshine and will be seen as very bright at night, while urban illumination is undetected.

IMAGE UNAVAILABLE FOR COPYRIGHT REASONS

A pass by NOAA-9 at 13.46 GMT, 12 September 1985, as seen by the channel 3 waveband, which is also in a water vapour window. Fires in which surplus straw is being burned on the farms of England after the harvest can be seen. Other, more regular hotspots are also recorded, such as steel works in Dunquerque and Scunthorpe, and flares on North Sea platforms. But urban areas do not show up at night as they would in a visible waveband (see ref. 2).

The figure shows the fires burning straw after the harvest on the farms of England in midday sunshine. Although channel 3 information was very often spoiled in the satellites before NOAA-7 by interference, later satellites have recorded it very well, and have been doing so for several years. A tape of the original digital message can usually give relative intensities, although big fires may saturate it. That could easily be remedied if it were required for hotspot surveys; and the resolution (pixel size 1.1 km at nadir) is much better than DMSP records. However, to record the message at full resolution it would require the receiver to be within the general area being surveyed, for example one station at about the centre of gravity of Africa.

A more satisfactory method for equatorial observation is to use a geostationary satellite; and there is a reasonable prospect that the next Meteosat, above the Equator on the zero meridian, will have a recording channel in the same wavelength band as channel 3. The message could then be made available everywhere in Europe and Africa at any time of day or night, so it would be possible to make the most of cloud-free periods.

R. S. Scorer
2 Stanton Rd,
London SW20 8RL, UK

1. Cahoon, D. R. *et al. Nature* **359**, 812–815 (1992).
2. Scorer, R. S. *Satellite as Microscope* (Ellis Horwood, Chichester, 1990).

University of Dundee

Homeobox genes and the zootype

SIR — Possession of a specific set of genes involved in pattern formation has been proposed as the character defining the kingdom Animalia (the zootype[1]). This concept arises from some remarkable similarities in terms of both structure and expression pattern between key development-regulating genes in relatively 'advanced' metazoans, specifically *Drosophila* and vertebrates. Comparative data for 'primitive' metazoans are required to validate the zootype concept and, as the most primitive metazoans with tissue-level organization, cnidarians are potentially one of the most informative 'lower' metazoan phyla. Here we demonstrate that *even-skipped* and *Antennapedia* class homeobox genes are adjacent in the genome of the coral *Acropora formosa*. This linkage in a cnidarian, observed also in vertebrates[2,3] (*a* in the figure), suggests first that this is likely to be the ancestral arrangement of these genes; and second that the 'primitive' function of *even-skipped* class genes is in posterior pattern formation.

We have isolated a single *A. formosa* genomic clone containing a pair of homeobox genes. Subclones derived from one end of this genomic clone encode a homeodomain belonging to the *even-skipped (eve)* class[4]. The similarity between the predicted amino-acid sequence of the cnidarian *eve*-like homeodomain and its insect and vertebrate equivalents is, remarkably, approximately 77–80 per cent (*b* in the figure), showing that this class of genes was distinct very early in

© 1993 Nature Publishing Group